Cleaner Materials 20 (2026) 100389

Contents lists available at ScienceDirect

Cleaner Materials

journal homepage: www.journals.elsevier.com/cleaner-materials

Chemo-physical rejuvenation of aged SBS-modified bitumen: Multiscale effects of oils, polymer replenishment, and reactive chain extender☆

Bowen Li [a,b], Xueyan Liu [a], Yvong Hung [c], Quentin Arnoux [c], Anthon Tolboom [d], Eyassu Hagos [e], Johannes Mirwald [b], Bernhard Hofko [b], Peng Lin [a,f,*]

[a] Section of Pavement Engineering, Department of Engineering Structures, Faculty of Civil Engineering and Geosciences, Delft University of Technology, Delft, the Netherlands
[b] Christian Doppler Laboratory for Chemo-Mechanical Analysis of Bituminous Materials, Institute of Transportation, TU Wien, Vienna, Austria
[c] Center de recherche de Solaize, TotalEnergies OneTech, Solaize, France
[d] Latexfalt BV, Koudekerk aan den Rijn, the Netherlands
[e] Boskalis Nederland BV, Rotterdam, the Netherlands
[f] Rijkswaterstaat, Ministry of Infrastructure and Water Management, Utrecht, the Netherlands

ARTICLE INFO

Keywords:
PmB
Regeneration
Spectroscopy
Rheology
Morphology
Reclaimed asphalt pavement (RAP)
High-value recycling

ABSTRACT

Styrene-butadiene-styrene (SBS)-modified binders in porous asphalt age rapidly, degrading both the viscoelastic bitumen phase and the crosslinked polymer network, hindering high-value recycling of reclaimed asphalt pavement (RAP). Conventional rejuvenation predominantly softens bitumen while overlooking polymer restoration. This study separates rejuvenation into two categories, *what* is repaired (bitumen vs SBS) and *how* it is repaired (physical vs chemical), to develop and compare four families: (1) oils targeting the bitumen phase, (2) oil–SBS blends supplying fresh polymer, (3) methylene diphenyl diisocyanate (MDI) promoting chemical reconnection of SBS chains, and (4) chemo-physical systems combining MDI with oil–SBS. Chemical properties were linked to performance using Fourier-Transformation Infrared (FTIR) spectroscopy, Gas Chromatography-Flame Ionization Detection (GC-FID), Dynamic Shear Rheometer (DSR) master curves, Multiple Stress Creep and Recovery Test (MSCRT), creep-relaxation, Linear Amplitude Sweep (LAS), fluorescence microscopy, and Environmental Scanning Electron Microscopy (ESEM). Results show that oils softened the binder and improved fatigue and low-temperature properties but diluted the SBS signal and failed to restore elasticity. Oil–SBS raised the SBS index and partially recovered elasticity, though microscopy revealed only discrete polymer domains. MDI on its own enhanced stiffness and elastic recovery but caused brittleness. Chemo-physical rejuvenators reconciled these trade-offs, yielding elasticity comparable to the unaged binder, creep-relaxation and LAS fatigue resistance approaching or exceeding the reference, and dense, well-dispersed polymer-rich domains. These findings highlight the need to combine bitumen softening, polymer replenishment, and chemical chain reconnection for effective SBS restoration and high-quality recycling of SBS-modified RAP, thereby advancing cleaner, resource-efficient pavement material systems.

Introduction

Since the 1980 s, over 85% of Dutch roads have used porous asphalt for its water permeability, noise reduction, and other environmental benefits (van Vilsteren, 2017; Gupta et al., 2019; Chen and Yang, 2020). However, its open structure accelerates aging, increasing binder brittleness, and causing ravelling (Gupta et al., 2019; Gupta, 2021). To improve durability, polymer-modified bitumen (PmB) is used to enhance adhesion and resist cracking and rutting (Gupta, 2021; Wang, 2015; Izaks, 2022). Among various modifiers, styrene–butadiene–styrene (SBS) is especially favored for its good compatibility with bitumen, effective performance, and cost-efficiency (Zhu et al., 2014). Like unmodified bitumen, SBS-modified bitumen also undergoes aging through exposure to heat, moisture, UV–visible radiation,

☆ This article is part of a special issue entitled: 'Pavement materials' published in Cleaner Materials.

* Corresponding author at: Section of Pavement Engineering, Department of Engineering Structures, Faculty of Civil Engineering and Geosciences, Delft University of Technology, Delft, the Netherlands.
E-mail addresses: peng.lin@rws.nl, P.Lin-2@tudelft.nl (P. Lin).

https://doi.org/10.1016/j.clema.2026.100389
Received 22 December 2025; Received in revised form 9 March 2026; Accepted 9 March 2026
Available online 13 March 2026

and atmospheric oxidants such as O_2, O_3, and NO_x, ultimately contributing to pavement deterioration (Han, 2022; Mirwald, 2022; Stüwe, 2025; Li, 2025). Over time, this results in large volumes of asphalt waste containing aged PmBs. Recycling such waste is crucial for reducing costs, conserving resources, and protecting the environment. However, due to performance concerns, many agencies limit the use of reclaimed asphalt, especially in surface layers (Leng, 2018). The systematic downcycling of high-value PmB into base layers constitutes a significant loss of engineered material performance and economic value, while accelerating virgin resource depletion and expanding the overall environmental footprint (van Bochove, 2020). To mitigate this issue, research has focused on rejuvenators that can restore the properties of aged PmB, thereby enabling its reuse without compromising performance.

While both the aged base bitumen phase and degraded SBS polymer phase should be addressed during rejuvenation, experimental studies rarely distinguish between their individual rejuvenation paths (Xing, 2023). Many focus solely on restoring the bitumen phase using oils, overlooking the polymer phase. Others combine fresh SBS with oils to target both phases. Some studies also explore reactive rejuvenators designed to directly repair degraded SBS.

Within this context, oils, particularly those derived from waste or bio-based sources, have been extensively investigated as practical rejuvenators, as they can effectively soften aged bitumen and improve rheology, but limitations remain in elasticity, thermal stability, and polymer repair (Chen, 2014). Tung oil improves high-temperature performance and low-temperature ductility, while waste cooking oil extends fatigue life (Yan, 2021). Aromatic oils outperform waste engine oil across strain levels, which only enhances fatigue resistance at large strain (Qiu, 2018). Cashew shell oil shows the best softening and durability for SBS-modified bitumen compared with vacuum steam oil, corn oil, and waste engine oil (Cao, 2019). Bio-rejuvenators further reduce asphaltenes and oxidative indices, though their effect is mainly physical and cannot restore degraded SBS networks (Zhu, 2017; Cai, 2019).

To address the degraded polymer phase, several studies have explored oil–SBS physical rejuvenators. Hong et al. and Eltwati et al. reported that blends of ~75% aromatic oil with ~25% SBS polymer not only softened aged binders but also improved ductility, softening point, and both low- and high-temperature performance, while FTIR spectroscopy confirmed partial recovery of the SBS related indices (Hong, 2020; Eltwati, 2022). Similar improvements in elasticity, ductility, and cracking resistance were achieved with rejuvenators combining aromatic oil, light oil, corn oil, and SBS polymer, with microscopy showing restoration of the polymer network structure (Cong et al., 2020). More complex formulations, incorporating stabilizers, dispersants, and petroleum resins, were also found to enhance bitumen's ductility, deformation resistance, and high/low temperature performance by dispersing light components and rebuilding the polymer network (Zhao et al., 2018). Finally, rejuvenators combining bio-oil, polymer modifiers, plasticizers, and crosslinking agents not only restored cracking resistance and elastic recovery but also extended fatigue life, with FTIR evidence of network structure reformation (Wang, 2021).

Besides conventional rejuvenators, reactive chemical rejuvenators are increasingly explored for SBS-modified bitumen. As SBS degrades, hydroxyl and carboxyl groups form at polymer fracture sites, allowing reactive compounds to reconnect chains (Han, 2021; Cao, 2020). Epoxy-based rejuvenators such as 1, 4-butanediol diglycidyl ether (BUDGE) and trimethylolpropane triglycidyl ether (TMPGE) improved ductility and cracking resistance, with BUDGE performing better; FTIR spectroscopy and microscopy confirmed chemical reactions with degraded SBS (Xu, 2017). Comparisons of BUDGE and methylene diphenyl diisocyanate (MDI) showed complementary effects – BUDGE enhanced ductility, viscosity, and fatigue resistance, while MDI improved elasticity and rutting resistance (Xu, 2017). Similarly, isocyanates including hexamethylene diisocyanate (HDI), MDI, and toluene-2, 6-diisocyanate (TDI) were found to raise softening point and viscoelasticity, with HDI favoring low-temperature resistance and MDI giving the best overall performance (Cao, 2020). Bio-based epoxidized soybean oil (ESO) activated by triphenyl phosphine (TPP) also reconnected degraded SBS segments, improving flexibility and viscoelasticity, though excessive catalyst reduced performance (Wei et al., 2020). Adding aromatic oil to ESO-TPP balanced softening and high-temperature stability (Wei et al., 2022). Finally, Li et al. developed a composite rejuvenator (fluid catalytic cracking slurry, C12-14 aliphatic glycidyl ether, MDI), which improved overall properties and low-temperature resistance, though with a slight loss in high-temperature stiffness (Li, 2019).

Although the rejuvenation effects of oils, added SBS polymer, and reactive additives such as MDI on aged SBS-modified binders have been reported in previous studies, existing work typically addresses these approaches in isolation or focuses on formulation-specific optimization. For example, while combinations of oil-based softening and chemical reconnection have been explored, such as oil–MDI binary systems, the explicit replenishment of the SBS polymer phase in conjunction with targeted chemical reconnection through an oil–SBS–MDI ternary system is rarely considered, despite the fact that polymer degradation is a key contributor to performance loss in aged SBS-modified binders. As a result, the respective roles of bitumen softening, polymer replenishment, and chemical reconnection remain difficult to disentangle. Moreover, existing studies employing isocyanate-based rejuvenators typically require dosages of 1% or higher to achieve noticeable polymer reconnection effects, and the potential for achieving efficient polymer restoration with minimal reactive additive content has not been systematically explored. To address this gap, the present study introduces a mechanistic framework that distinguishes rejuvenation strategies based on both the phase being repaired (bitumen versus SBS polymer) and the restoration mechanism employed (physical versus chemical). In this framework, physical rejuvenation refers to non-reactive polymer phase restoration via physical fresh polymer replenishment, whereas chemical rejuvenation refers to reactive mechanisms involving covalent interactions with degraded polymer chains. Using this framework, oil-based, physical (oil–SBS), chemical (MDI), and chemo-physical rejuvenation strategies incorporating fresh SBS polymer and targeted chemical reconnection are systematically compared under identical aging and dosage conditions. Notably, the chemo-physical systems employ only 0.5% MDI in combination with oil–SBS blends, demonstrating that limited chemical intervention can yield substantial restoration of polymer-related viscoelastic behavior. MDI is employed as a representative chemical rejuvenator to illustrate this category, while other chemical repair mechanisms reported in the literature fall within the same conceptual framework but are beyond the scope of the present study. The goal is to establish a more complete rejuvenation strategy that not only softens the aged bitumen but also repairs and rebuilds the SBS polymer network, thereby offering a pathway toward practical, durable, and sustainable RAP recycling. By integrating bio-based oils with minimal chemical intervention (0.5% MDI), this chemo-physical strategy mitigates RAP downcycling, facilitating high-value material recovery and the development of cleaner, resource-efficient pavement systems.

Materials and methods

Materials

The SBS-modified bitumen used in this study was supplied by TotalEnergies Bitumen. Its laboratory-measured empirical properties in the unaged state are summarized in Table 1.

Three oils were selected to represent distinct chemical characteristics and interaction potentials with bitumen and SBS polymer. The aromatic oil is predominantly hydrocarbon-based with low polarity and relatively high viscosity, making it effective in softening the bitumen matrix and promoting swelling of the SBS polymer through physical absorption.

Table 1
Empirical properties of the SBS-modified binder in unaged state.

Property	Value	Test Method
Penetration 25 °C (0.1 mm)	81	EN 1426
Penetration Class	40–100 (Class 5)	EN 14023
Softening Point (°C)	74.6	EN 1427
Softening Point Class	≥ 70 (Class 4)	EN 14023
Elastic Recovery 25 °C (%)	93	EN 13398
Elastic Recovery Class	≥ 80 (Class 2)	EN 14023
135 °C Viscosity (Pa•s)	2.50	EN 13302

Rapeseed oil, a triglyceride-based bio-oil with moderate polarity and viscosity, contains oxygen-containing functional groups that may influence its interaction with aged bitumen and facilitate polymer swelling. Tall oil, containing fatty acids and resin acids with higher polarity and lower viscosity, was selected due to its strong softening capability and favorable affinity with the SBS phase. This selection enables systematic evaluation of how oil chemistry and rheological characteristics affect bitumen softening, SBS swelling, and the overall rejuvenation response of aged SBS-modified binders. The properties of oils used in this study have been summarized in Table 2.

In addition to oil selection, a linear SBS polymer (Table 3) and an MDI (Table 4) were chosen based on practical and literature-supported considerations. Linear SBS was selected because of its simpler molecular architecture and lower resistance to flow compared with radial SBS, facilitating dispersion and swelling during blending and rejuvenation under laboratory and field-relevant mixing conditions. MDI was selected as a representative chemical rejuvenator due to its commercial availability, ease of handling, and well-documented reactivity toward functional groups present in aged bitumen and SBS polymers. Previous studies have demonstrated that isocyanate-based additives can effectively promote polymer reconnection and enhance elastic response in aged SBS-modified binders, making MDI a suitable model compound for investigating chemo-physical rejuvenation mechanisms (Han, 2021; Cao, 2020; Xu, 2017; Xu, 2025). During aging, SBS polymers undergo chain scission and oxidation, leading to the formation of hydroxyl and carboxyl functional groups. The isocyanate groups (–NCO) in MDI can react with these functionalities to form urethane- and/or amide-type linkages, thereby reconnecting degraded polymer segments and contributing to partial restoration of polymer network integrity (Xu, 2025; Chattopadhyay and Raju, 2007).

Aging and rejuvenation methods

The SBS-modified binder was aged using the Thin Film Oven Test (TFOT) at 163 °C for 5 h in accordance with EN 12607-2 (CEN, 2014), followed by the Pressure Aging Vessel (PAV) aging at 100 °C and 2.1 MPa according to EN 14769 (CEN, 2023). A total of four PAV cycles (80 h) were applied to simulate long-term aging representative of porous asphalt mixtures.

Based on the ingredients discussed in the previous section, four types of rejuvenators were prepared for this study. The oil rejuvenators consisted of a single oil component. The physical rejuvenators were produced by blending SBS polymer into oil using a high-shear mixer at 185 °C and 3000 rpm for 40 min, followed by mixing with an overhead stirrer at 180 °C and 800 rpm for 2 h to ensure sufficient polymer swelling in the oil (Li, 2023). The chemical rejuvenator contained pure MDI, while the chemo-physical rejuvenator combined MDI with the physical rejuvenator; the two components were stored separately to avoid premature reactions. Table 5 listed all the samples contained in this study. The dosages of oils and MDI were selected to enable systematic comparison rather than formulation optimization. Preliminary screening showed that oil dosages above 10% caused excessive softening, while varying oil dosages to equalize performance would obscure mechanistic differences. Similarly, MDI dosages were chosen to highlight contrasts between physical, chemical, and chemo-physical rejuvenation strategies under comparable conditions. To produce rejuvenated bitumen, the 4PAV-aged binder was portioned into small metal cans, dosed with the designed amount of rejuvenator by weight percent, and mixed thoroughly using a hand-held mixer at 170 °C for 15 min. The resulting rejuvenated binder was then poured onto silicone paper for subsequent testing. Fig. 1 demonstrated the production processes of physical rejuvenators, and the rejuvenation processes with different types of rejuvenators.

Table 2
Properties of oils used in this study.

Oil	Viscosity at 20 °C (Pa•s)	Density at 20 °C (g/cm^3)
Aromatic oil	0.817	0.955
Rapeseed oil	0.160	0.915
Tall oil	0.093	0.927

Table 3
Properties of Kraton D1101 linear SBS used in this study.

Property	Value
Supplied form	Powder dusted with amorphous silica
Polystyrene content	31%
Specific gravity	0.94

Table 4
Properties of BASF IsoPMDI used in this study.

Property	Value
Chemical name	Isocyanic acid, polymethylenepolyphenylene ester
CAS number	9016–87-9
Form	Liquid
Boiling point	330 °C
Specific gravity	1.22

Table 5
Explanation of rejuvenated binder names, corresponding rejuvenation types, and rejuvenator used.[a]

Rejuvenation type	Sample name	Explanation[b]
–	Unaged	Unaged SBS-modified binder
–	4PAV	Four PAV cycles aged SBS-modified binder
Oil	10%Aro	+10% aromatic oil
Oil	10%Rap	+10% rapeseed oil
Oil	10%Tall	+10% tall oil
Physical	10%Aro-SBS	+10% physical rejuvenator[c] (Aro-SBS)
Physical	10%Rap-SBS	+10% physical rejuvenator[c] (Rap-SBS)
Physical	10%Tall-SBS	+10% physical rejuvenator[c] (Tall-SBS)
Chemical	10%MDI	+10% MDI
Chemo-physical	9.5%Aro-SBS + 0.5%MDI	+9.5% physical rejuvenator (Aro-SBS) + 0.5% MDI
Chemo-physical	9.5%Rap-SBS + 0.5%MDI	+9.5% physical rejuvenator (Rap-SBS) + 0.5% MDI
Chemo-physical	9.5%Tall-SBS + 0.5%MDI	+9.5% physical rejuvenator (Tall-SBS) + 0.5% MDI

[a] SBS refers to the styrene–butadiene–styrene polymer added via the rejuvenator formulation. The base binder is an SBS-modified bitumen.
[b] All rejuvenated binders are based on the four-PAV-cycles aged SBS-modified binder.
[c] Physical rejuvenator = oil–SBS blend containing 75 wt% oil and 25 wt% SBS polymer.

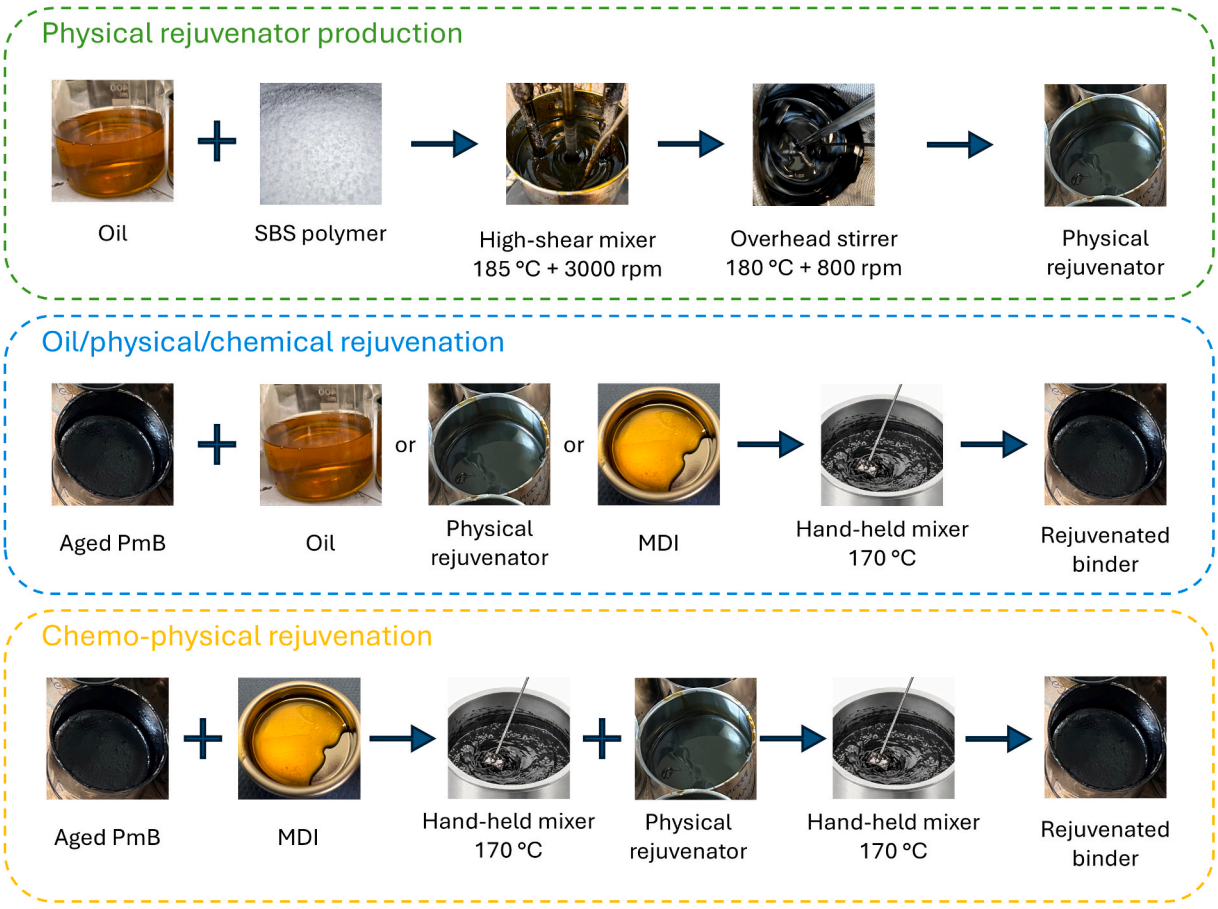

Fig. 1. Schematic diagram of physical rejuvenator production and rejuvenation processes.

Analysis methods

Attenuated Total Reflectance Fourier-Transformation Infrared (ATR-FTIR) spectroscopy

A Thermo Scientific Nicolet iS50 FTIR spectrometer equipped with an attenuated total reflectance (ATR) module was used for chemical analysis. Spectra were collected in the 4000–400 cm^{-1} wavenumber range with a resolution of 4 cm^{-1} and 32 scans. Prior to each measurement, a background spectrum was collected. A small amount of bitumen was then taken from the silicone paper using a clean spatula and placed directly onto the ATR crystal and ensured full contact. Four replicate measurements were performed for each binder. After each measurement, the ATR crystal was thoroughly cleaned with acetone to avoid cross-contamination between samples.

Spectra were analyzed with Bruker's OPUS software. After applying min–max normalization over the 3200–2800 cm^{-1} wavenumber range, tangential valley-to-valley integration was performed for polybutadiene (PB) and polystyrene (PS) peaks as follows:

- PB_{FTIR}: 983–950 cm^{-1}
- PS_{FTIR}: 708–690 cm^{-1}

The SBS indices SBS_{FTIR} were then calculated with the following equation:

$$SBS_{FTIR} = PB_{FTIR} + PS_{FTIR} \tag{1}$$

Gas Chromatography-Flame Ionization Detection (GC-FID)

For GC-FID analysis, 15 mg of bitumen was dissolved in 1.0 mL cyclohexane in a 2 mL vial and heated for 5 min. A 0.5 µL cyclohexane blank was first injected into a Thermo Scientific TRACE 1300 GC-FID device for zero calibration, followed by 0.5 µL of sample. The column oven was programmed from 90 to 430 °C at 10 °C/min, with the FID held at 450 °C. Gas flow rates were 35 mL/min (H_2), 350 mL/min (air), and 40 mL/min (makeup), using helium as the carrier gas at 20 mL/min. GC-FID results are presented as normalized detector signal (a.u.) versus retention time (min).

Dynamic Shear Rheometer (DSR)

An Anton Paar Modular Compact Rheometer MCR502 was used for rheological analysis, following the DSR setup, zero-gap setting, and sample preparation and mounting procedures in EN 14770 (CEN, 2012). Frequency sweep tests were conducted at temperatures of 0, 15, 30, 40, 60, and 80 °C with a frequency range of 0.1 to 10 Hz.

Complex modulus master curves were constructed using the Sigmoidal model from the National Cooperative Highway Research Program (NCHRP) Project A-37A, and phase angle master curves were derived via Kramers-Kronig relations, with 30 °C as the reference temperature (Yusoff, 2013; Oshone, 2017; Lin, 2021). The corresponding equations are shown below.

$$\log|G^*| = \upsilon + \frac{\alpha}{1 + e^{(\beta+\gamma\log\omega)}} \tag{2}$$

$$\delta = 90 \times \frac{dlogG^*}{dlog\omega} = -90 \times \alpha\gamma \frac{e^{(\beta+\gamma\log\omega)}}{[1 + e^{(\beta+\gamma\log\omega)}]^2} \tag{3}$$

where $|G^*|$ is the complex modulus (Pa), δ is the phase angle (°), ω is the reduced frequency at the reference temperature (rad/s), υ is the lower

asymptote, α is the difference between the values of the upper and lower asymptote, β and γ define the shape between the asymptotes and the location of the inflection point (inflection point obtained from $10^{(\beta/\gamma)}$).

The multiple stress creep and recovery test (MSCRT) was performed at 70 °C with a 25 mm spindle and 1 mm gap following EN 16659 (CEN, 2015). A temperature of 70 °C was selected to enhance sensitivity to polymer-related elastic recovery in SBS-modified binders and polymer-containing rejuvenation systems, as lower temperatures (e.g., 60 °C) were found to provide insufficient differentiation between formulations. During the testing, the sample was subjected to stresses of 0.1 kPa and 3.2 kPa, respectively, for 1 s before receiving 9 s to recover. The tests were executed 30 times, and the specification described above was used to compute the average percent recovery R.

The creep-relaxation test was conducted at 0 °C using an 8 mm spindle and 2 mm gap. Samples were loaded with 1% shear strain in 0.1 s and allowed 100 s relaxation, with stress recorded at a rate of 100 points per second to capture the rapid initial response (Jing, 2020).

The linear amplitude sweep (LAS) tests followed AASHTO TP 101–14 at 20 °C with an 8 mm spindle and 2 mm gap (AASHTO, 2014). A frequency sweep (0.1% strain, 0.2–30 Hz) determined the damage parameter α, followed by an amplitude sweep (0–30% strain at 10 Hz). The calculation of the LAS results adhered to the aforementioned standard.

Fluorescence microscopy

For microscopy analysis, ~75 mg of preheated, homogenized bitumen was poured into a slide cavity on a 150 °C heating plate to form a flat surface. Four replicates were prepared per binder. Slides were removed within 30 s to minimize aging, covered with metal lids to avoid contamination and light exposure, then cooled to room temperature for ≥30 min to stabilize microstructure formation.

Surface morphological analysis was performed using a Nikon Optical Inverse Microscope (OIM) equipped with brightfield, darkfield, and fluorescence modes. The system included a motorized Märzhäuser X-Y-Z stage, epifluorescence unit, Nikon DS-Fi3 camera, Nikon CFI TU Plan BD ELWD 100× objective (NA/WD: 0.80/4.5 mm), and a CoolLED pE-4000 light source with 16 selectable LEDs (365–770 nm). The epifluorescence unit was fitted with three filter blocks, including a custom fluorescence filter (403/95 nm excitation, 500 nm long-pass emission, 495 nm dichroic).

Image acquisition was carried out with Nikon NIS-Elements AR. A z-stack (±10 µm) was recorded and merged into fully focused composites. Brightfield mode (500 nm LED, 5 ms) was first used to focus while minimizing light-induced aging, followed by fluorescence imaging (435 nm LED, 900 ms) (Mirwald, 2022). One fluorescence image per sample was captured, yielding four images per binder. Captured RGB fluorescence images were converted to 16-bit grayscale in Fiji (ImageJ) to enhance contrast and highlight microstructural features.

Environmental Scanning Electron Microscopy (ESEM)

Cylindrical sample holders (8 mm in diameter) were prepared for ESEM examination. Binders were heated at 150 °C for 30 min; approximately 0.1 g of each material was then transferred to a holder with a spatula, flattened on a 170 °C hotplate for ~60 s, and stored at 10 °C overnight prior to imaging.

Microstructural observations were performed at 25 °C using an environmental scanning electron microscope (ESEM) at the TotalEnergies OneTech Solaize Research Center (ANA@CRES, France). Imaging conditions were as follows: accelerating voltage (HV) 30.00 kV, chamber pressure 1.30 mbar, working distance (WD) 9.8 mm, and spot size 3.5. The microscope operated in secondary-electron (SE) mode with a gaseous secondary electron detector (GSED). Images were acquired at nominal magnifications of 250×, 500×, and 1000×; scale bars were adjusted accordingly (40 µm for the 500 × images unless otherwise specified) (Lin, 2021; Mikhailenko et al., 2017). Each binder was imaged in three non-overlapping fields of view, and three replicate measurements were collected on the same day to ensure reproducibility.

Results and discussion

This chapter first examines the effects of different rejuvenators on chemical properties, followed by their influence on rheological characteristics and, finally, on morphological features. Together, these analyses provide a comprehensive understanding of the performance of the various rejuvenators.

Effects on chemical properties

FTIR spectroscopy

The FTIR spectra in Fig. 2 reveal distinct chemical differences among the unaged, aged, and rejuvenated SBS-modified binders. As expected, the 4PAV-aged binder shows a notable increase in absorbance in the carbonyl region (1746–1666 cm^{-1}), the sulfoxide region (1066–984 cm^{-1}), and the polarity-sensitive range (1330–1130 cm^{-1}), indicating oxidation and a shift in chemical composition toward more polar fractions such as resins and asphaltenes (Mirwald, 2020).

Upon rejuvenation, particularly with rapeseed and tall oils, the absorbance in these regions increases even further. This is primarily attributed to the intrinsic functional groups present in bio-based oils, including ester carbonyls from triglycerides and other oxygenated compounds that contribute to both the carbonyl and C–O stretching bands (Vlachos, 2006). In contrast, the petroleum-derived aromatic oil induces only moderate spectral changes, consistent with its hydrocarbon-rich and low-polarity chemical nature. When SBS polymer is incorporated into the oil, the resulting physical rejuvenators exhibit reduced intensity of oil-related FTIR bands. This attenuation is partly associated with the lower absolute oil content in the formulation, but also reflects physical interactions between oil and SBS, such as polymer swelling and partial encapsulation of oil components within the polymer-rich phase, which reduce their direct contribution to the FTIR signal. These differences highlight the distinct chemical contributions of each rejuvenator type and their varying degrees of interaction with both the aged base bitumen matrix and the SBS polymer phase.

The FTIR spectra in Fig. 3 illustrate the chemical effects of MDI-based rejuvenation on the 4PAV-aged SBS-modified binder. In addition to the previously discussed absorption bands, several new peaks are observed in the MDI-containing samples. The peak at 1526 cm^{-1} corresponds to N–H bending, while the bands at 1311 cm^{-1} and 1219 cm^{-1} are assigned to C–N stretching vibrations, all of which are commonly referred to as amide bands in FTIR studies of bitumen and polymer systems (Xu, 2017). In the context of isocyanate chemistry, however, such peaks can arise from several types of linkages: most likely urethane bonds formed by the reaction of –NCO with hydroxyl groups (–OH), and possibly amide bonds formed by the reaction of –NCO with carboxyl groups (–COOH) accompanied by CO_2 release. Urea-type linkages (–NCO + $–NH_2$) are generally less relevant here, as SBS itself does not generate free $–NH_2$ groups upon degradation unless nitrogen-containing stabilizers or additives are present. Thus, the observed FTIR peaks provide strong evidence for the formation of urethane- and/or amide-type linkages between MDI and oxidized SBS fragments, supporting the conclusion that MDI contributes to partial restoration of the degraded polymer network.

The SBS index derived from FTIR in Fig. 4 offers a quantitative estimate of the relative presence of SBS polymer segments, specifically polybutadiene (PB) and polystyrene (PS) blocks, in the binder matrix. As expected, the unaged binder shows a relatively high SBS index (~3.3), reflecting the intact polymer phase. After long-term aging, the SBS index decreased noticeably, confirming degradation of the polymers. In the

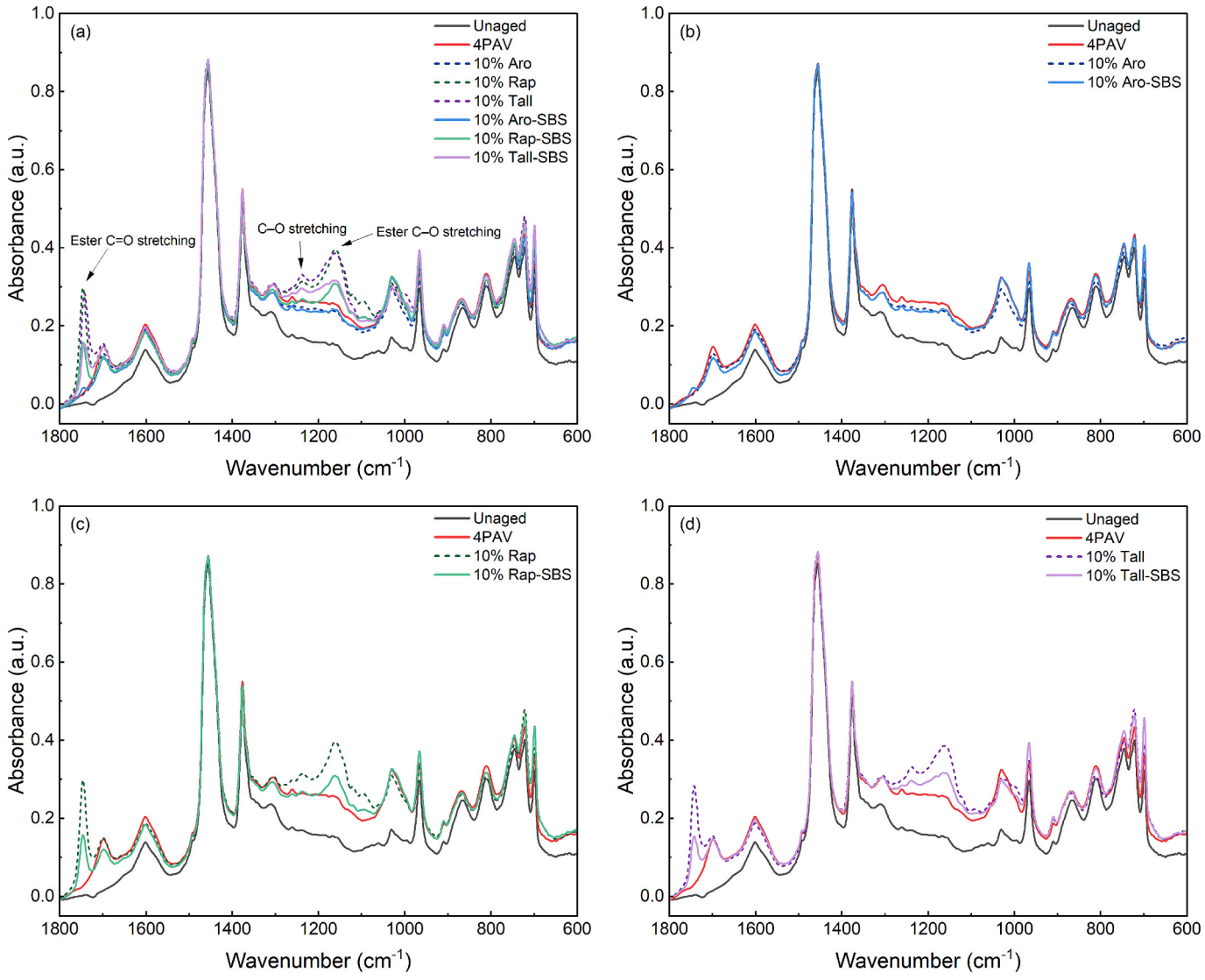

Fig. 2. FTIR spectra of unaged, 4PAV-aged, and rejuvenated binders by oil and physical rejuvenators in key fingerprint regions.

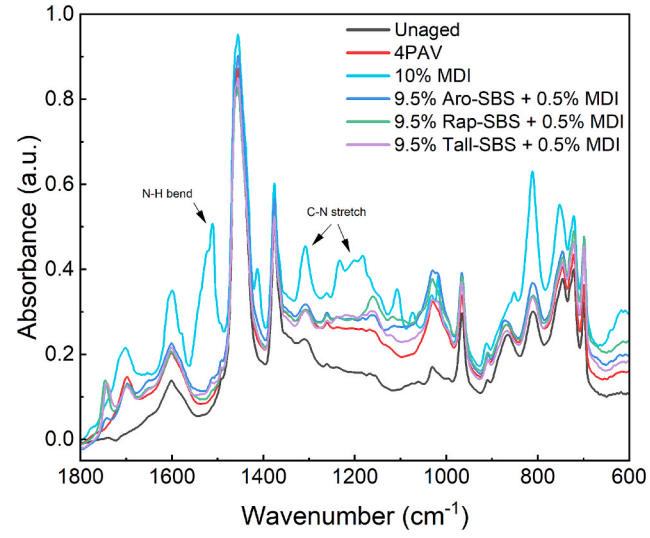

Fig. 3. FTIR spectra of unaged, 4PAV-aged, and rejuvenated binders by chemical and chemo-physical rejuvenators in key fingerprint regions.

case of binders rejuvenated with pure oils, the SBS index remains low (~2.8–2.9) and even lower than that of the aged binder. This suggests that while these oils may soften the aged binder, they also dilute the remaining SBS polymer phase, reducing its relative signal in the FTIR spectrum without chemically restoring it. By contrast, the physical rejuvenators exhibit a significant increase in the SBS index, exceeding the unaged reference in all cases. This enhancement is primarily due to the contribution of fresh SBS introduced through the rejuvenator formulation, which remains chemically intact and detectable by FTIR. Although all physical rejuvenators contain the same SBS content, the Tall-SBS system shows the highest SBS index, suggesting improved detectability or dispersion of the polymer phase. This may be due to the favorable compatibility between tall oil and SBS, as tall oil contains both polar and non-polar components that can improve the swelling and stabilization of SBS chains in the bitumen matrix. Such interactions may reduce SBS aggregation and enhance its FTIR response. However, it should be noted that FTIR spectroscopy primarily reflects chemical functionalities associated with SBS segments and does not, by itself, provide a direct measure of polymer network integrity or mechanical connectivity. The binder treated with 10% MDI alone exhibits an SBS index of 3.3, which is notably higher than that of the aged 4PAV binder and comparable to the unaged reference. This improvement indicates that MDI can chemically react with degraded SBS segments, contributing to partial restoration of

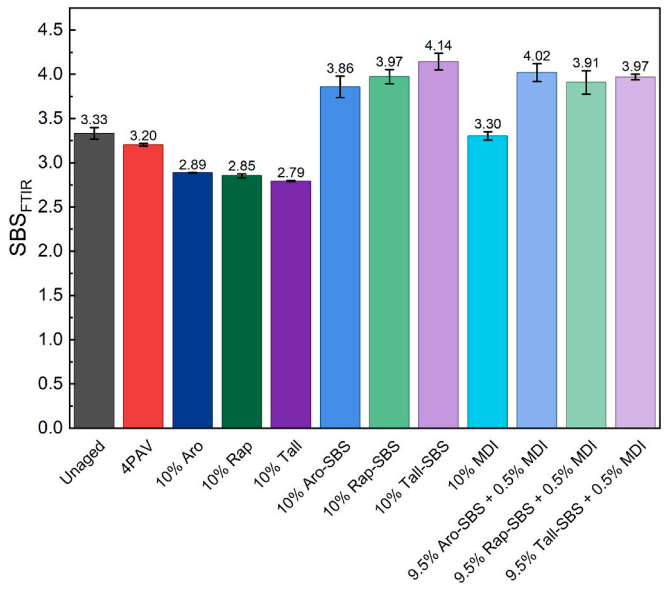

Fig. 4. FTIR SBS index of unaged, 4PAV-aged, and rejuvenated binders with different rejuvenators.

the polymer structure. In the chemo-physical rejuvenation systems, where 0.5% MDI is first reacted with the aged binder and then blended with physical rejuvenators, the SBS index of all three combinations converges to a similar value (~3.9–4.0). This convergence suggests that pre-reacting MDI with the aged binder improves the baseline condition of the polymer phase, enabling more consistent incorporation and detection of the fresh SBS added later via the physical rejuvenators. In other words, by stabilizing or partially restoring the aged SBS in advance, MDI reduces variability caused by differences in oil-polymer compatibility. As a result, the added SBS is more uniformly dispersed or better retained across all systems, leading to a reliable and elevated FTIR response regardless of oil type.

GC-FID

The GC-FID chromatograms of the unaged and 4PAV-aged binders in Fig. 5 show similar overall profiles, but with notable differences in intensity across the retention window of ~18–32 min. After aging, the binder exhibits a slightly lower signal intensity in this region, indicating a reduction in lighter and mid-range volatiles, likely due to oxidative degradation and volatilization during prolonged thermal aging.

As confirmed by Wang's study, the strong early peak (~10–15 min) in the pure aromatic oil GC-FID curve (see Appendix A, Fig.A.1.) can be attributed to abundant alkylbenzenes, which are typical constituents of petroleum-derived aromatic oils (Wang et al., 1994). In the aromatic oil-rejuvenated binder (Fig. 5(b)), this peak appears as a broader plateau, which reflects the same group of light aromatics observed in the oil but modified due to dilution, dispersion, and matrix interaction with the aged binder. The GC-FID profile of the rapeseed oil-rejuvenated binder (Fig. 5(b)) shows a distinct group of sharp peaks between 20 and 23 min, which are absent in the aged binder. These peaks correspond to volatile oxygenated compounds introduced by the rapeseed oil, such as aldehydes, ketones, and short-chain alcohols, formed through fatty acid oxidation. As reported by Rao et al., compounds like hexanal, 2,3-butanedione, and 1-pentanol are abundant in rapeseed oil and align with this retention range (Rao, 2024). The GC-FID chromatogram of the tall oil-rejuvenated binder reveals a sharp peak at ~18–19 min, followed by a cluster of signals between 20 and 24 min (Fig. 5(b)). The initial peak likely corresponds to unsaturated long-chain fatty acids, primarily oleic and linoleic acid, which are known to dominate the composition of tall oil fatty acids (TOFA) and elute in this range under typical GC conditions (McGuire and Powis, 1998). The subsequent group of peaks aligns with the elution range of resin acids, such as abietic, dehydroabietic, and isopimaric acids, commonly present in distilled tall oil (McGuire and Powis, 1998; Jenab, 2014). Compared to the petroleum-based aromatic oil, which shares chemical similarity with the aged binder and thus shows better compatibility, the two bio-oils introduce more distinct and polar compounds that are less miscible with the bitumen matrix. This chemical dissimilarity might increase the risk of phase separation or segregation during storage or service.

Compared to the binders rejuvenated with pure oils, the oil–SBS rejuvenated systems show a clear reduction in the characteristic oil peaks and a notable increase in signal intensity between 25 and 34 min (Fig. 5(c)). The suppression of oil-related peaks likely results from reduced volatility or physical entrapment of oil components within the polymer-rich SBS phase, as also seen in the previous FTIR results (Fig. 2). Meanwhile, the elevated late-retention signals are attributed to higher molecular weight SBS-derived fragments and oligomers (Rødland, 2022). In addition to these molecular changes, the presence of SBS may also enhance the compatibility and dispersion of the oil within the aged binder, reducing the risk of segregation during storage or service.

The binder rejuvenated with pure MDI could not be tested due to excessive stiffness. In the chemo-physical rejuvenated binders, the GC-FID curves show a further reduction in oil-related peaks and a higher signal beyond 25 min compared to the physical rejuvenator system (Fig. 5(d)). Since MDI was added and reacted first with the aged binder, these changes are attributed to its reaction with degraded SBS chains, forming higher molecular weight urethane- and/or amide-type linkages. This more structured polymer phase may trap or immobilize later-added oil components, reducing their volatility. The elevated late-retention signals align with the presence of larger MDI-SBS reaction products and are consistent with the additional FTIR peaks at 1526, 1311, and 1219 cm^{-1}, confirming chemical bonding between isocyanate groups and degraded polymer fragments.

Overall, the GC-FID results indicate that rejuvenator performance is closely linked to changes in oil volatility and retention behavior. Pure oil rejuvenators introduce a higher fraction of volatile and mid-retention components, which may contribute to effective bitumen softening but appear to remain weakly associated with the SBS phase. In contrast, oil–SBS systems show a suppression of oil-related volatile peaks and an increased late-retention signal, suggesting physical entrapment of oil components within the swollen polymer phase and reduced volatility. In chemo-physical systems, the further shift toward higher retention times may reflect the formation of higher-molecular-weight polymer structures through chemical reconnection, which could stabilize the oil within the polymer-rich domains and enhance polymer network functionality.

Effects on rheological properties

Complex modulus and phase angle master curves

Fig. 6 presents the complex modulus and phase angle master curves of unaged, 4PAV-aged, and rejuvenated binders using oils and physical rejuvenators. The unaged binder exhibits a pronounced downward trend and plateau region in the phase angle curve, characteristic of an intact polymer network. After aging, these features disappeared, indicating polymer degradation. In parallel, the complex modulus increased substantially, reflecting oxidative hardening and the loss of volatile components.

With pure oil rejuvenators, the complex modulus decreased, with tall oil showing the strongest softening effect, nearly restoring the stiffness level to the unaged binder. In contrast, the phase angle curves of oil-rejuvenated binders displayed a more viscous response, but the characteristic downward trend and plateau region were not recovered, confirming that oils cannot restore the degraded polymer network. The addition of SBS polymer as a physical rejuvenator slightly increased

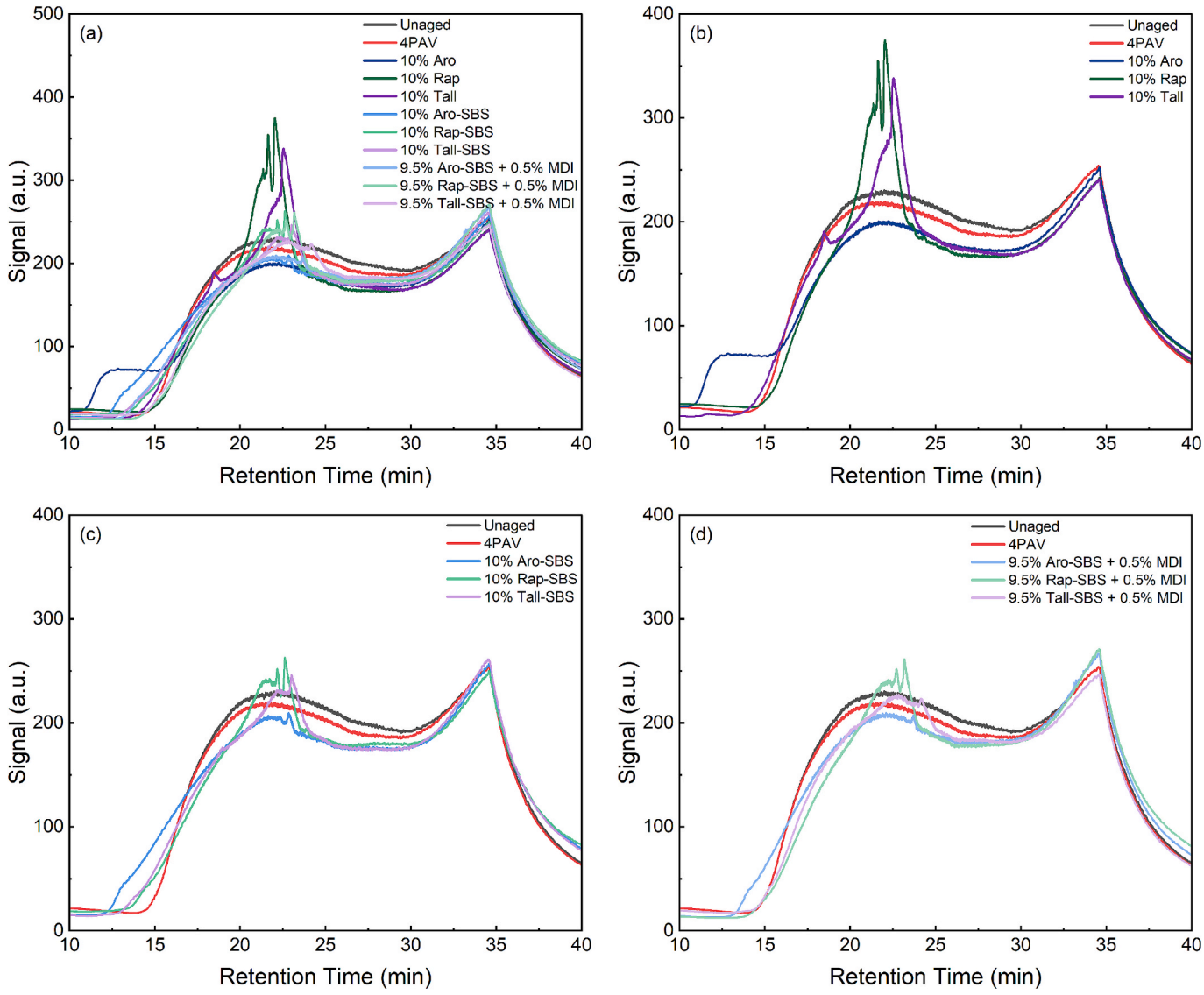

Fig. 5. GC-FID chromatogram of unaged, 4PAV-aged, and rejuvenated binders with different rejuvenators.

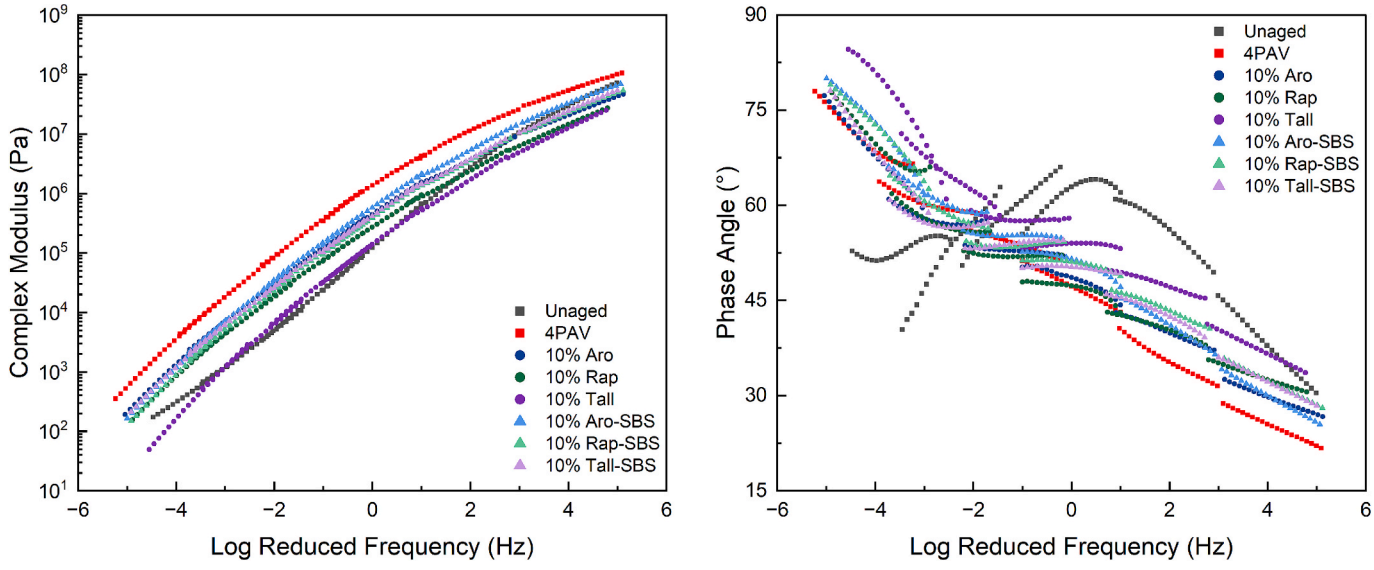

Fig. 6. Complex modulus and phase angle master curves of unaged, 4PAV-aged, and rejuvenated binders by oil and physical rejuvenators.

stiffness compared to oils alone. Although the SBS index derived from FTIR suggests that the rejuvenated binders contain a higher amount of SBS-related chemical signatures than the unaged reference, this increase is not reflected in the phase angle master curves. Only a slight plateau reappears in the intermediate frequency range, indicating that polymer-related viscoelastic features are only partially recovered and that the restoration of a mechanically effective polymer network remains limited. This discrepancy highlights that FTIR-derived SBS indices primarily capture the presence of characteristic polymer-related chemical functionalities, including contributions from degraded or newly added polymer fragments, rather than the integrity or connectivity of the polymer network. Rheological measurements are therefore essential to evaluate the physical functionality of the polymer network, including its load-bearing efficiency and elastic response, and should be interpreted in conjunction with chemical indicators rather than as direct proxies for network performance.

Fig. 7 shows the complex modulus and phase angle master curves of binders rejuvenated with chemical and chemo-physical rejuvenators. The chemical rejuvenator alone significantly increased binder stiffness and elasticity, which may enhance high-temperature performance but could compromise fatigue resistance and low-temperature cracking behavior. When combined with physical rejuvenators, these negative effects were mitigated, resulting in all three blends exhibiting similar complex modulus and phase angle values. The downward shift and pronounced plateau in the phase angle curves highlight the strong effect of the reactive chain extender – compared with the previously discussed physical rejuvenators, replacing only 0.5% of the formulation with a chemical chain connector produced a disproportionately large change in viscoelastic response. However, despite partial restoration of the polymer phase, the overall viscoelastic behavior of the rejuvenated binders remained noticeably different from that of the unaged binder. The curves were generally shifted to lower positions, reflecting a more elastic response, which may adversely impact binder performance at low and intermediate temperatures.

MSCRT

The shear strain–time responses at a stress level of 3.2 kPa and 70 °C provide direct insight into the binders' resistance to permanent deformation under repeated creep–recovery loading (Fig. 8).

Binders rejuvenated with pure oils exhibit pronounced strain accumulation over successive cycles, forming a steep staircase-shaped response. This behavior indicates a dominant non-recoverable deformation component and poor resistance to rutting at high temperature, with the tall oil–rejuvenated binder showing the most severe strain growth. Incorporating SBS into the oils reduces the rate of strain accumulation, confirming that the added polymer contributes to improved elastic response; however, substantial creep growth remains, indicating that the restored polymer structure is still insufficiently connected to effectively limit permanent deformation. In contrast, binders containing MDI, either alone or in combination with physical rejuvenators, show very limited strain accumulation and small, stable creep–recovery loops. This response reflects a predominantly elastic deformation mechanism and a strong resistance to permanent deformation, consistent with the formation of a chemically reconnected polymer network. These trends are quantitatively confirmed by the percent recovery values ($R_{3.2kPa}$) summarized in Fig. 8. All binders rejuvenated with pure oils showed low recovery, confirming poor elastic response and insufficient polymer phase restoration. Slight improvements were observed in the physical rejuvenator systems, suggesting that added SBS contributes some physical elasticity. Among them, the Tall-SBS system achieved the highest recovery, consistent with its higher SBS index observed in FTIR, indicating better retention or integration of the added polymer phase. In contrast, binders containing MDI, either alone or in combination with physical rejuvenators, achieved R values above 94%, effectively matching the unaged binder. This confirms that chemical restoration using MDI is highly effective in re-establishing the elastic characteristics of the aged PmB. The synergy between MDI and SBS ensures strong elasticity recovery, likely due to MDI's chemical interaction with degraded SBS chains and resulting crosslink reformation.

Creep-relaxation

The creep-relaxation results in Fig. 9 assess the binders' response to rapid loading and their ability to dissipate stress at low temperature. Lower maximum shear stress and shorter stress relaxation time both indicate better resistance to low-temperature cracking. Binders rejuvenated with pure oils show the lowest stress values and fastest stress relaxation, suggesting superior low-temperature flexibility and cracking resistance, though likely at the cost of elasticity and structural integrity. The physical rejuvenated binders display moderately higher stiffness and relaxation times, indicating partial recovery of elastic behavior while still retaining acceptable low-temperature flexibility. The binder with 10% MDI alone shows the highest stress and longest relaxation time, reflecting a highly stiff and elastic structure, but poor performance

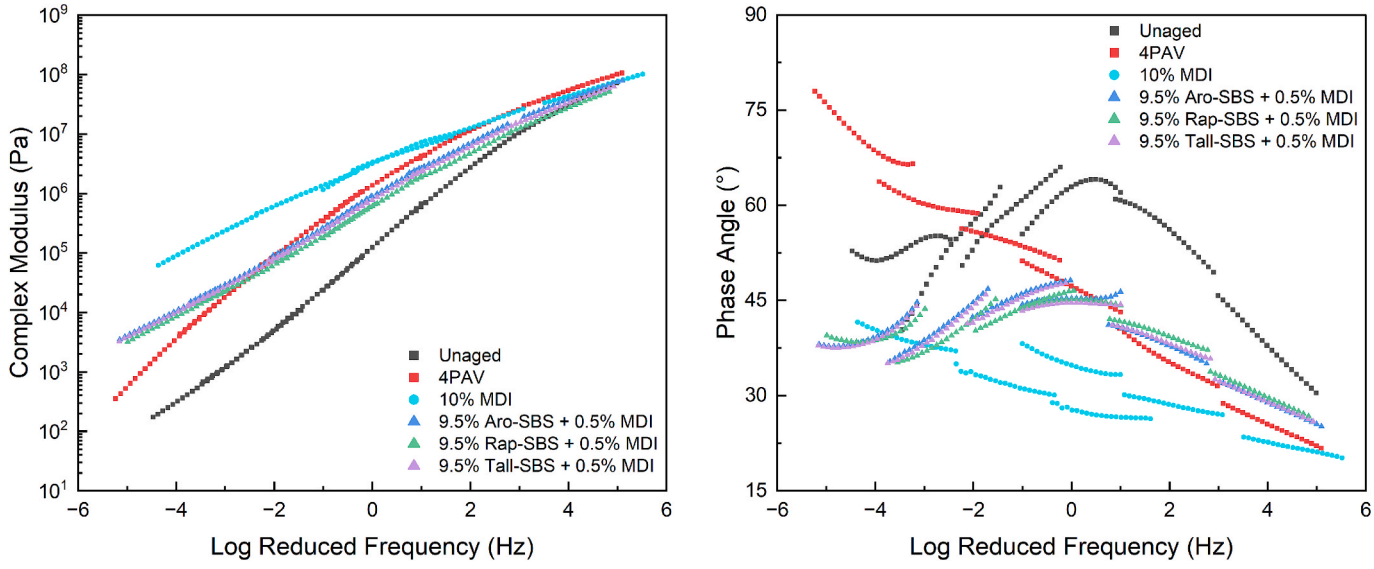

Fig. 7. Complex modulus and phase angle master curves of unaged, 4PAV-aged, and rejuvenated binders by chemical and chemo-physical rejuvenators.

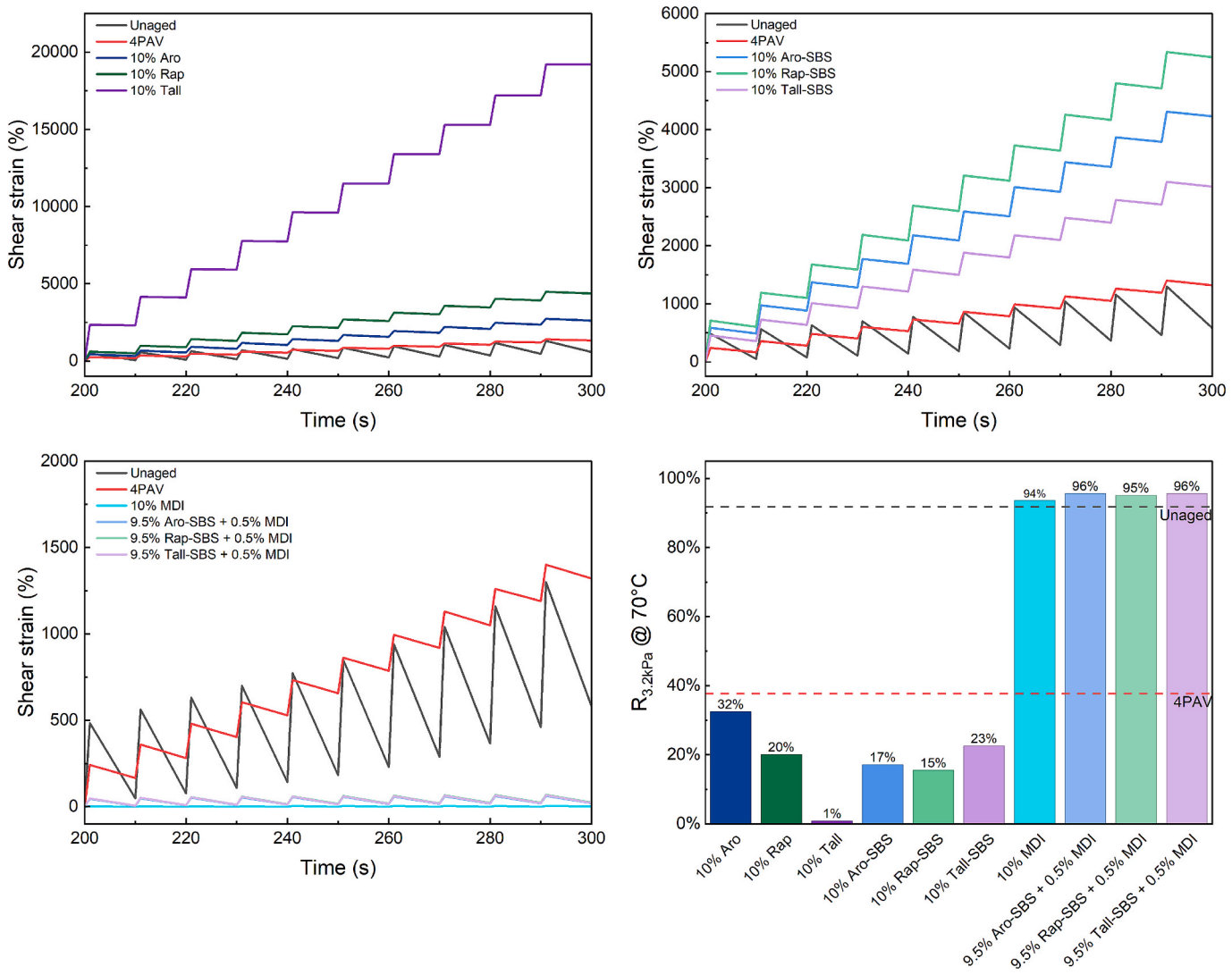

Fig. 8. Shear strain curves at 3.2 kPa shear stress and percent recovery $R_{3.2kPa}$ at 70 °C from MSCRT of unaged, 4PAV-aged, and rejuvenated binders with different rejuvenators.

in cracking resistance due to insufficient stress dissipation. In contrast, the chemo-physical rejuvenator systems achieved intermediate values, closely matching the unaged binder. This indicates that the combined system restores elasticity while maintaining adequate low-temperature flexibility, offering the best balance of performance across the test conditions.

LAS

The LAS stress–strain curves (Fig. 10(a)) confirm the strong stiffening of the 4PAV binder, with the highest peak stress and rapid failure, while the unaged binder maintains lower stress and better ductility. Pure oils reduce the peak stresses substantially, with tall oil showing the lowest values and thus the greatest improvement in ductility and fatigue tolerance. When SBS is introduced into the oils, the curves shift upward, reflecting a moderate increase in stiffness compared to pure oils but still much lower than the aged reference. Among the physical rejuvenators, Rap-SBS and Tall-SBS achieve lower peaks and smoother relaxation, suggesting a more favorable balance between strength and ductility. Overall, physical rejuvenators enhance elasticity relative to oils alone but maintain lower stresses than the aged binder, pointing to partial restoration of polymer-like behavior without excessive brittleness. Fig. 10(b) shows that 10% MDI produces the highest peak stress, even above the aged binder, reflecting strong stiffness recovery but poor ductility. In contrast, the chemo-physical rejuvenators display lower peak stresses and smoother post-peak declines, indicating a more balanced response. Among them, 9.5% Tall-SBS + 0.5% MDI sustains strain the longest, suggesting improved ductility compared to the aromatic or rapeseed oil-based blends. Overall, MDI alone leads to excessive stiffness, while combining it with physical rejuvenators moderate brittleness and better restores polymer-related viscoelastic behavior.

The 4PAV-aged binder (Fig. 10(c)) exhibits a higher fatigue life than the unaged binder at small strain levels, which can be attributed to its extreme stiffness. However, as strain increases, its fatigue life quickly falls below that of the unaged binder, reflecting its brittleness under severe deformation. Rejuvenation with pure oils reduces fatigue life at small strains but enhances it at larger strains, with tall oil showing the best performance at moderate-high strains, consistent with its softer and more ductile response observed in the stress–strain curves. Incorporating SBS into the oils (physical rejuvenators) slightly hardens the binders, which raises fatigue life at small strains but reduces it somewhat at larger strains. Nonetheless, all rejuvenated binders outperform the aged reference across the strain range. When MDI is used alone, the binder becomes extremely stiff, leading to a sharp increase in fatigue life at small strains but a marked reduction at large strains (Fig. 10(d)). By contrast, combining MDI with physical rejuvenators balances this

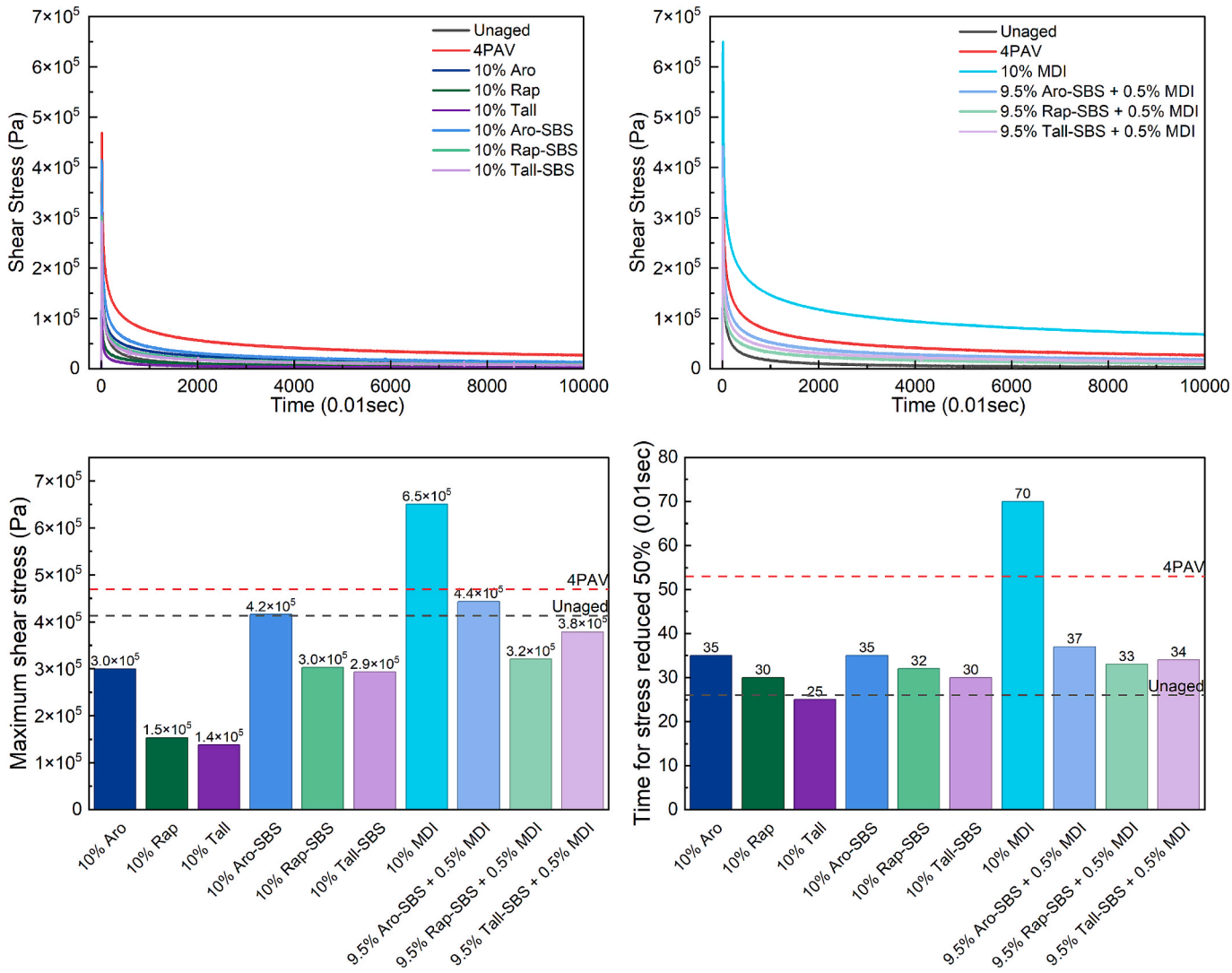

Fig. 9. Relaxation curves, maximum shear stress, and time for stress reduced 50% from creep-relaxation test of unaged, 4PAV-aged, and rejuvenated binders with different rejuvenators.

excessive stiffness, resulting in consistently higher fatigue life than the aged binder, with the rapeseed and tall oil-based chemo-physical rejuvenators delivering the most favorable performance.

Effects on morphological properties

Fluorescence microscopy

Fig. 11 presents fluorescence microscopy images of the unaged, 4PAV-aged, and rejuvenated binders treated with different rejuvenators. The unaged binder exhibits a heterogeneous microstructure characterized by a dense, fine, and well-connected polymer network. After four PAV cycles, this morphology becomes blurred and poorly defined, with the surface dominated by so-called bee and *peri*-phase structures and only a few isolated polymer dots remaining. This observation indicates severe oxidation of the base bitumen and substantial degradation of the SBS polymer network (Li, 2025).

Rejuvenation with pure oils primarily softens the binder surface; however, bee and *peri*-phase structures still dominate the microstructure, and a continuous polymer network is not recovered. Compared with the aged binder, a larger number of discrete polymer dots becomes visible after oil treatment. This effect does not imply direct restoration of the polymer phase by the oil, but rather reflects surface softening of the highly aged binder, which allows residual polymer domains that were previously masked by surface hardening to become visible again, despite the fact that most of the original polymer network has already degraded (Li, 2025). Among the three oils, the two bio-oil rejuvenated binders exhibit a higher number of visible polymer dots than the aromatic oil-rejuvenated binder, suggesting a stronger softening effect of the bio-oils. In the oil–SBS rejuvenated binders, bright, spherical polymer-rich domains are clearly observed. Among these systems, the Tall-SBS rejuvenated binder shows the most uniformly dispersed polymer domains, indicating improved compatibility between tall oil and SBS. Treatment with MDI alone results in a microstructure that appears similar to the 4PAV-aged binder at first glance; however, closer inspection reveals a noticeably higher number of bright, dense polymer dots, suggesting partial restoration of the polymer phase through chemical bonding between isocyanate groups and degraded SBS fragments. The chemo-physical rejuvenators produce the most pronounced morphological transformation, characterized by numerous, finely dispersed polymer-rich domains. This uniform distribution highlights a synergistic mechanism: the oil component swells both aged and fresh SBS, while MDI chemically reconnects degraded polymer segments, together yielding the most advanced microstructural restoration among all rejuvenation strategies.

It should be noted that the observed polymer morphology is also

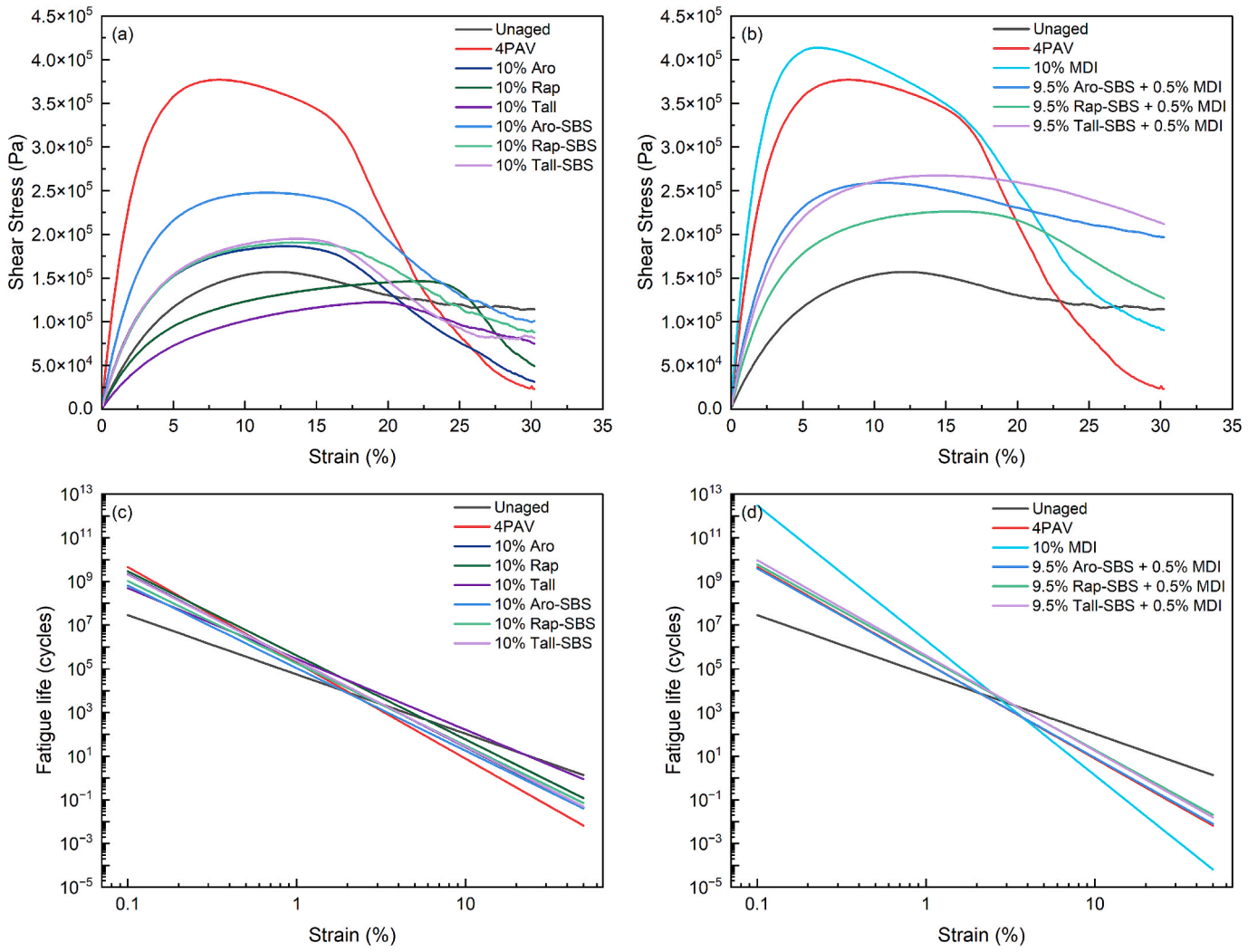

Fig. 10. Stress–strain and fatigue life from LAS test of unaged, 4PAV-aged, and rejuvenated binders with different rejuvenators.

influenced by the blending procedure. In this study, rejuvenators were incorporated using manual blending, which restricts polymer dispersion and makes it difficult to achieve a fully connected network comparable to that of a commercially produced SBS-modified binder. This approach was intentionally adopted to better reflect practical rejuvenation conditions at the mixture level, where blending times and conditions in batch plants are typically very limited.

ESEM

Fig. 12 shows the ESEM micrographs of unaged, 4PAV-aged, and rejuvenated binders with different rejuvenators. The unaged binder displays a thick, dense, well-connected network of fibrils, forming a continuous and ordered morphology. After 4PAV aging, the fibrillar network is no longer observable and is replaced by a diffuse, granular surface, indicating severe oxidation, surface hardening, and an increase in the molecular weight of the bitumen (Mikhailenko et al., 2017).

Rejuvenation with oils is able to reintroduce fibrillar structures, but their morphology differs depending on the oil type. Aromatic oil produces poorly defined fibrils with rough, irregular surfaces, whereas the two bio-oils (rapeseed and tall oil) generate clearer and more connected networks with smoother fibril surfaces. The smoother appearance likely reflects an oil-rich coating or wetting of fibrils and the aged bitumen matrix, which is consistent with the stronger C=O and C–O bands detected in FTIR (from fatty/resin acids and esters) and with the mid-retention components observed in GC-FID. Binders rejuvenated with oil–SBS blends (physical rejuvenators) exhibit bubble-like features distributed on the fibril surfaces, likely corresponding to the added SBS polymer. Unlike in the unaged binder, these SBS particles do not fully fuse into the fibrillar network, suggesting limited compatibility with the aged bitumen. Interestingly, the Tall-SBS sample shows noticeably smaller bubbles compared to the other oils, which may indicate that tall oil enhances the compatibility and dispersion of the newly added polymer. Rejuvenated binder with pure MDI was not suitable for ESEM imaging due to excessively hard surface. Finally, the chemo-physical rejuvenator (9.5% Tall-SBS + 0.5% MDI as a representative due to device limitation) displays a highly rugged morphology with thickened, vertically aligned fibril bundles. This may result from additional surface hardening induced by MDI or from side products of chemical reactions between isocyanate groups and degraded polymer fragments.

Conclusions

This study investigated the rejuvenation of severely aged SBS-modified binders using a two-dimensional framework that distinguishes (i) which phase is repaired (bitumen versus SBS polymer) and (ii) how restoration is achieved (physical versus chemical mechanisms). Oils, oil–SBS physical rejuvenators, a reactive di-isocyanate (MDI), and chemo-physical combinations were systematically evaluated using complementary chemical, rheological, and morphological techniques.

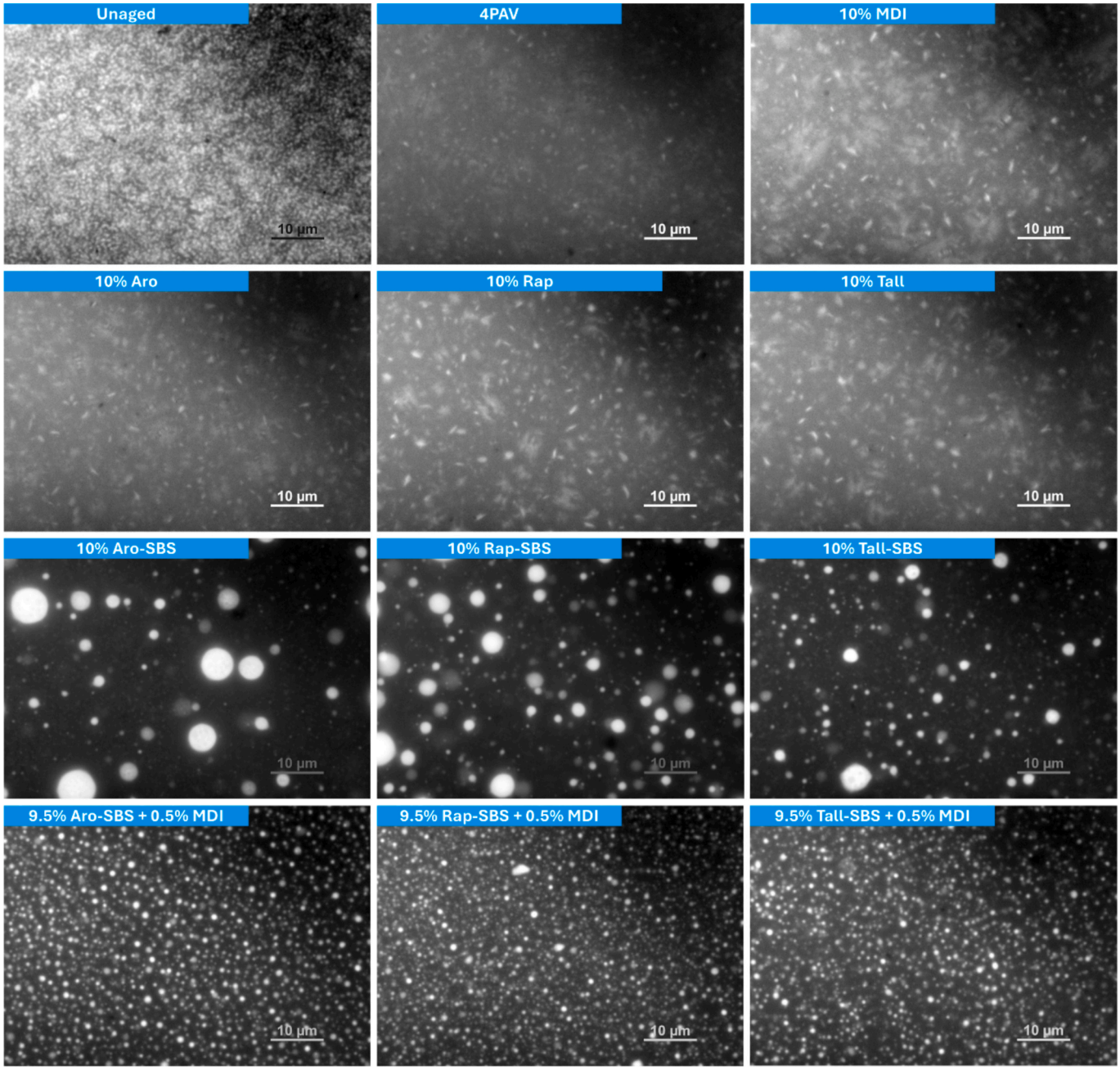

Fig. 11. Fluorescence microscopy images of unaged, 4PAV-aged, and rejuvenated binders with different rejuvenators.

On this basis, the following conclusions can be drawn:

- Rejuvenators targeting only the bitumen phase (aromatic and bio-oils) effectively softened the aged binder and improved low-temperature flexibility and fatigue resistance, but failed to restore polymer-related elasticity. Oil–SBS physical rejuvenators increased the SBS-related chemical signal and provided partial elastic recovery; however, rheological and morphological results indicate that the re-formed polymer domains remained weakly connected and mechanically inefficient.
- Chemical rejuvenation using MDI alone promoted strong stiffness and elastic recovery but resulted in a brittle response with reduced ductility and cracking resistance. In contrast, chemo-physical rejuvenation combining a physical rejuvenator with only a small amount of MDI (0.5%) produced a markedly improved balance of properties, with a pronounced restoration of the phase angle plateau and a downward shift of the master curves, highlighting the high efficiency of targeted chemical reconnection.
- Among the investigated oils, tall oil showed the strongest softening effect and the most favorable interaction with the SBS polymer, reflected by reduced stiffness, higher elastic recovery, elevated SBS indices, and more uniform polymer dispersion. The 9.5% Tall-SBS + 0.5% MDI system is presented as a representative example of the chemo-physical concept, demonstrating that effective SBS restoration requires the concurrent action of bitumen softening, polymer replenishment, and limited chemical reconnection rather than optimization of a single formulation.

Overall, the results confirm that polymer restoration cannot be achieved by chemical or physical approaches alone. Efficient rejuvenation of aged SBS-modified binders requires a chemo-physical strategy that combines limited chemical intervention with practical physical

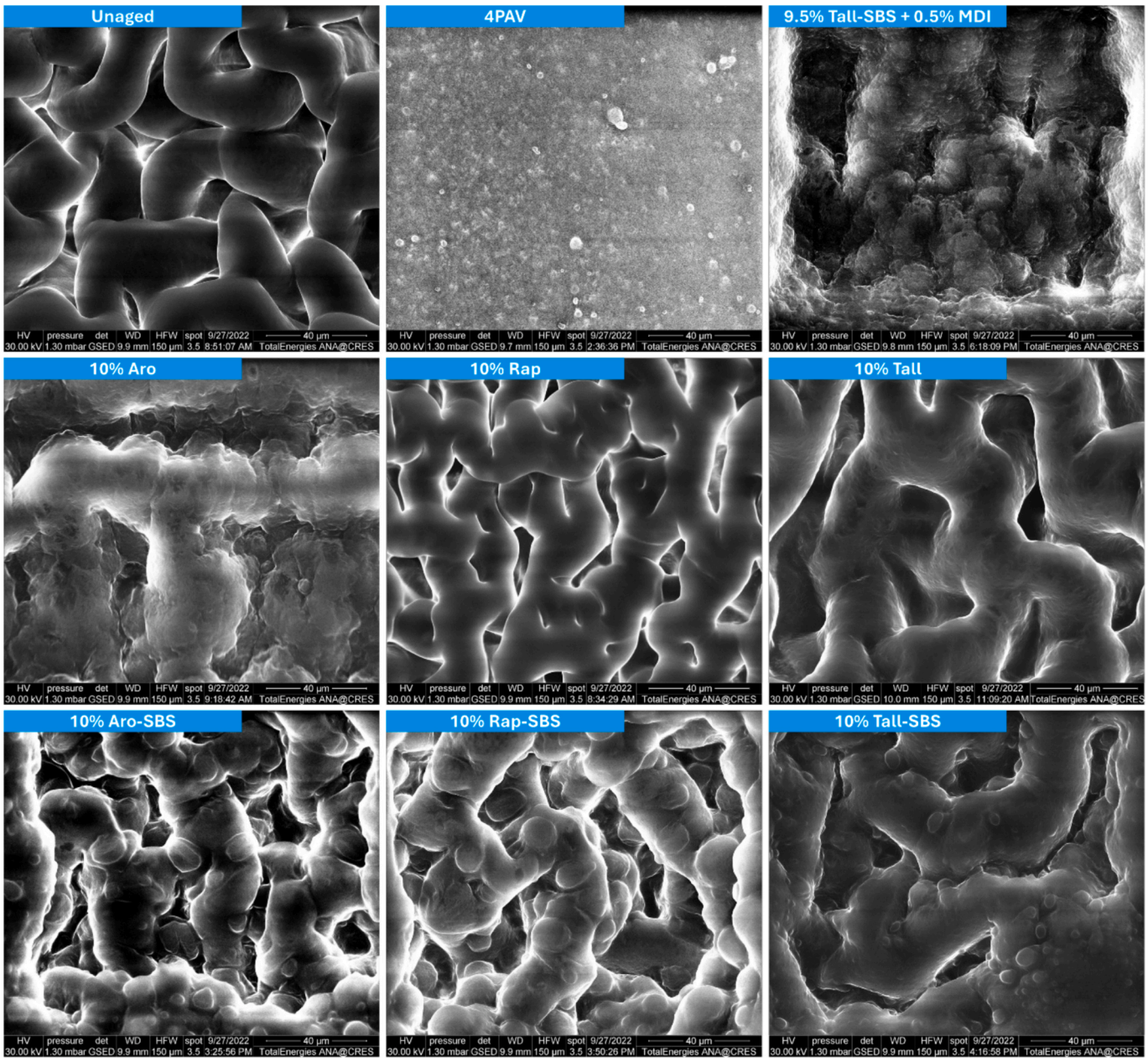

Fig. 12. ESEM images of unaged, 4PAV-aged, and rejuvenated binders with different rejuvenators.

rejuvenation, offering a realistic pathway for high-quality recycling of SBS-modified RAP under field-relevant mixing conditions. By achieving effective polymer restoration with minimal chemical intervention, this chemo-physical strategy extends pavement service life and maximizes resource efficiency, directly advancing cleaner construction practices. Although the proposed chemo-physical systems achieved partial recovery of the polymer phase, the resulting viscoelastic response remained distinct from that of the unaged binder, with systematically shifted rheological curves and persistent differences in key performance indicators. These residual gaps, together with observed deviations in morphology, highlight the need for further optimization. Future work will focus on refining formulation and dosage, improving network connectivity to better balance elasticity and ductility, assessing long-term aging resistance, and validating the proposed concepts at mastic and mixture scales.

Declaration of Generative AI and AI-assisted technologies in the writing process

During the preparation of this work the author(s) used ChatGPT in order to improve the readability and language of the manuscript. After using this tool, the author(s) reviewed and edited the content as needed and take(s) full responsibility for the content of the published article.

CRediT authorship contribution statement

Bowen Li: Writing – original draft, Visualization, Investigation, Formal analysis, Data curation. **Xueyan Liu:** Writing – review & editing, Methodology, Funding acquisition, Conceptualization. **Yvong Hung:** Writing – review & editing, Resources, Investigation. **Quentin Arnoux:** Writing – review & editing, Investigation. **Anthon Tolboom:** Writing – review & editing, Resources, Investigation. **Eyassu Hagos:** Writing – review & editing, Resources, Investigation. **Johannes Mirwald:** Writing – review & editing, Validation, Methodology, Formal analysis.

Bernhard Hofko: Writing – review & editing, Validation, Methodology, Formal analysis. **Peng Lin:** Writing – review & editing, Supervision, Methodology, Conceptualization.

Funding

This work is part of the project "Rejuvenator Recycling of Polymer Modified Asphalt Concrete (RePoMA)" under Cooperation Agreement C21-087 between Delft University of Technology, TotalEnergies OneTech, and Latexfalt BV. The research was financially supported by TotalEnergies OneTech and Latexfalt BV.

Declaration of competing interest

The authors declare that they have no known competing financial interests or personal relationships that could have appeared to influence the work reported in this paper.

Appendix A

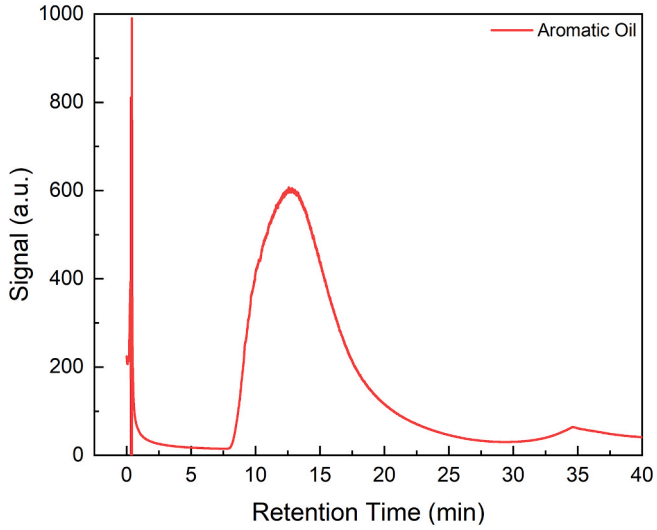

Fig. A.1. . GC-FID chromatogram of pure aromatic oil.

Data availability

Data will be made available on request.

References

AASHTO, TP 101 Standard Method of Test for Estimating Damage Tolerance of Asphalt Binders Using the Linear Amplitude Sweep. 2014.

Cai, X., et al., 2019. Internal aging indexes to characterize the aging behavior of two bio-rejuvenated asphalts. J. Clean. Prod. 220, 1231–1238.

Cao, Z., et al., 2019. Effect of different rejuvenators on the rheological properties of aged SBS modified bitumen in long term aging. Constr. Build. Mater. 215, 709–717.

Cao, Z., et al., 2020. Preparation and characterization of active rejuvenated SBS modified bitumen for the sustainable development of high-grade asphalt pavement. J. Clean. Prod. 273, 123012.

CEN, EN 14770 Bitumen and bituminous binders - Determination of complex shear modulus and phase angle - Dynamic Shear Rheometer (DSR). 2012.

CEN, EN 12607-2 Bitumen and bituminous binders - Determination of the resistance to hardening under influence of heat and air - Part 2: TFOT method. 2014.

CEN, EN 16659 Bitumen and Bituminous Binders - Multiple Stress Creep and Recovery Test (MSCRT). 2015.

CEN, EN 14769 Bitumen and bituminous binders - Accelerated long-term ageing conditioning by a Pressure Ageing Vessel (PAV). 2023.

Chattopadhyay, D.K., Raju, K.V.S.N., 2007. Structural engineering of polyurethane coatings for high performance applications. Prog. Polym. Sci. 32 (3), 352–418.

Chen, M., et al., 2014. Physical, chemical and rheological properties of waste edible vegetable oil rejuvenated asphalt binders. Constr. Build. Mater. 66, 286–298.

Chen, J.-S., Yang, C.H., 2020. Porous asphalt concrete: a review of design, construction, performance and maintenance. Int. J. Pavement Res. Technol. 13 (6), 601–612.

Cong, P., Guo, X., Mei, L., 2020. Investigation on rejuvenation methods of aged SBS modified asphalt binder. Fuel 279, 118556.

Eltwati, A., et al., 2022. Synergistic effect of SBS copolymers and aromatic oil on the characteristics of asphalt binders and mixtures containing reclaimed asphalt pavement. Constr. Build. Mater. 327, 127026.

Gupta, A., et al., 2021. Critical assessment of new polymer-modified bitumen for porous asphalt mixtures. Constr. Build. Mater. 307, 124957.

Gupta, A., Rodriguez-Hernandez, J., Castro-Fresno, D., 2019. Incorporation of additives and fibers in porous asphalt mixtures: a review. Materials 12 (19), 3156.

Han, X., et al., 2021. Effects of reactive chain extension rejuvenation systems on the viscosity–temperature characteristics, rheological properties, and morphology of aged styrene–butadiene–styrene-modified bitumen. ACS Sustain. Chem. Eng. 9 (48), 16474–16484.

Han, X., et al., 2022. Development of novel composite rejuvenators for efficient recycling of aged SBS modified bitumen. Fuel 318, 123715.

Hong, W., et al., 2020. Investigation of rejuvenation and modification of aged asphalt binders by using aromatic oil-SBS polymer blend. Constr. Build. Mater. 231, 117154.

Izaks, R., et al., 2022. Performance properties of high modulus asphalt concrete containing high reclaimed asphalt content and polymer modified binder. Int. J. Pavement Eng. 23 (7), 2255–2264.

Jenab, E., et al., 2014. Production of renewable hydrocarbons from thermal conversion of abietic acid and tall oil fatty acids. Energy Fuel 28 (11), 6988–6994.

Jing, R., et al., 2020. Rheological, fatigue and relaxation properties of aged bitumen. Int. J. Pavement Eng. 21 (8), 1024–1033.

Leng, Z., et al., 2018. Value-added application of waste PET based additives in bituminous mixtures containing high percentage of reclaimed asphalt pavement (RAP). J. Clean. Prod. 196, 615–625.

Li, Z., et al., 2019. Assessment on physical and rheological properties of aged SBS modified bitumen containing rejuvenating systems of isocyanate and epoxy substances. Materials 12 (4), 618.

Li, B., 2023. Recycling of SBS Asphalt Mixture with Polymer Network Reconstructive Rejuvenators, in Faculty of Civil Engineering & Geosciences. TU Delft, Delft.

Li, B., et al., 2025. Characterizing the diversity of PmB aging with application to pavements. Fuel 400, 135803.

Lin, P., et al., 2021. ESEM observation and rheological analysis of rejuvenated SBS modified bitumen. Mater. Des. 204, 109639.

McGuire, J.M., Powis, P.J., 1998. Gas Chromatographic Analysis of Tall Oil Fractionation Products after Methylation with N,N-dimethylformamide dimethylacetal. J. Chromatogr. Sci. 36 (2), 104–108.

Mikhailenko, P., Kadhim, H., Baaj, H., 2017. Observation of bitumen microstructure oxidation and blending with ESEM. Road Mater. Pavement Des. 18 (sup2), 216–225.

Mirwald, J., et al., 2020. Understanding bitumen ageing by investigation of its polarity fractions. Constr. Build. Mater. 250, 118809.
Mirwald, J., et al., 2022. Impact of UV–Vis light on the oxidation of bitumen in correlation to solar spectral irradiance data. Constr. Build. Mater. 316, 125816.
Oshone, M., et al., 2017. Prediction of phase angles from dynamic modulus data and implications for cracking performance evaluation. Road Mater. Pavement Des. 18 (sup4), 491–513.
Qiu, Y., et al., 2018. Damage characteristics of waste engine oil bottom rejuvenated asphalt binder in the non-linear range and its microstructure. Constr. Build. Mater. 174, 202–209.
Rao, W., et al., 2024. Investigation of the quality of rapeseed oil derived from different varieties and growth periods based on GC-IMS technique. Microchem. J. 205, 111357.
Rødland, E.S., et al., 2022. A novel method for the quantification of tire and polymer-modified bitumen particles in environmental samples by pyrolysis gas chromatography mass spectroscopy. J. Hazard. Mater. 423, 127092.
Stüwe, S., et al., 2025. Influence of reactive oxygen species and humidity on binder aging under direct and indirect exposure. Mater. Struct. 58 (10), 342.
van Bochove, G., et al., 2020. High-quality reuse of polymer modified Asphalt. *7th Eurasphalt and Eurobitume Congress*.
van Vilsteren, I., 2017. Porous Asphalt - Dutch experiences with Porous Asphalt pavements. Conference of European Directors of Roads (CEDR).
Vlachos, N., et al., 2006. Applications of Fourier transform-infrared spectroscopy to edible oils. Anal. Chim. Acta 573–574, 459–465.
Wang, L., et al., 2015. Microstructure and rheological properties of aged and unaged polymer-modified asphalt binders. Road Mater. Pavement Des. 16 (3), 592–607.
Wang, T., et al., 2021. Rheological properties of aged bitumen rejuvenated by polymer modified bio-derived rejuvenator. Constr. Build. Mater. 298, 123249.
Wang, Z., Fingas, M., Li, K., 1994. Fractionation of a light crude oil and identification and quantitation of aliphatic, aromatic, and biomarker compounds by GC-FID and GC-MS, Part II. J. Chromatogr. Sci. 32 (9), 367–382.
Wei, C., Zhang, H., Duan, H., 2020. Effect of catalytic-reactive rejuvenator on structure and properties of aged SBS modified asphalt binders. Constr. Build. Mater. 246, 118531.
Wei, C., Zhang, H., Duan, H., 2022. The behaviour of rejuvenated SBS-modified asphalt incorporating catalytic-reactive compounded rejuvenator. Road Mater. Pavement Des. 23 (2), 433–444.
Xing, C., et al., 2023. Minireview on the rejuvenation of aged styrene–butadiene–styrene (SBS) modified bitumen: state-of-the-Art and Outlook. Energy Fuel 37 (11), 7634–7647.
Xu, X., et al., 2017. Effect of reactive rejuvenators on structure and properties of UV-aged SBS modified bitumen. Constr. Build. Mater. 155, 780–788.
Xu, X., et al., 2017. Structure and performance evaluation on aged SBS modified bitumen with bi- or tri-epoxy reactive rejuvenating system. Constr. Build. Mater. 151, 479–486.
Xu, X., et al., 2025. Material characterization and engineering performance evaluation of phosphogypsum as a high-performance filler for bituminous pavements. Fuel 393, 134977.
Yan, K., et al., 2021. Mechanical performance of asphalt rejuvenated with various vegetable oils. Constr. Build. Mater. 293, 123485.
Yusoff, N.I.M., et al., 2013. Modelling the rheological properties of bituminous binders using mathematical equations. Constr. Build. Mater. 40, 174–188.
Zhao, M., Shen, F., Ding, Q., 2018. Micromechanism of the Dispersion Behavior of Polymer-Modified Rejuvenators in Aged Asphalt Material. Appl. Sci. 8 (9), 1591.
Zhu, H., et al., 2017. Recycling long-term-aged asphalts using bio-binder/plasticizer-based rejuvenator. Constr. Build. Mater. 147, 117–129.
Zhu, J., Birgisson, B., Kringos, N., 2014. Polymer modification of bitumen: advances and challenges. Eur. Polym. J. 54, 18–38.